Polym. Bull. (2010) 65:395–409
DOI 10.1007/s00289-010-0293-y

ORIGINAL PAPER

Structure and properties of silk fibroin/carboxymethyl chitosan blend films

Jianxin He · Yan Wang · Shizhong Cui · Yaying Gao · Shanyuan Wang

Received: 31 October 2009 / Revised: 19 January 2010 / Accepted: 12 May 2010 /
Published online: 22 May 2010

Abstract The secondary structure of silk fibroin (SF) and the compatibility of the two components were associated with the carboxymethyl chitosan (CMCS) content in SF/CMCS blend films. A rather complete conformation transition of SF from random coil to β-sheet occurred after adding 5% CMCS into the SF film, and the blend film exhibited a high crystallinity and a good compatibility. The conformation of SF changed from β-sheet to α-helix when blending 10% CMCS. When the CMCS content was up to 15%, the conformation of SF in blend films showed a transformation from β-sheet to a random coil and their crystallinities decreased evidently; accordingly, there was a two-phase separation structure for the blend films containing 15% CMCS or more. However, the intermolecular interaction between the two polymers still existed in blend film with 15% CMCS or more. The blend films with 5–10% CMCS content showed the lower moisture absorption, swelling capacity, and solubility in water. These properties of blend films increased when adding CMCS more than 15%.

Keywords Silk fibroin film · Carboxymethyl chitosan · Conformation · Property

J. He · Y. Gao · S. Wang
College of Textiles, Donghua University, Shanghai 201620, People's Republic of China

J. He · Y. Wang · S. Cui
Henan Key Laboratory of Textile Materials, Zhongyuan University of Technology, Zhengzhou City 450007, People's Republic of China

J. He (✉)
College of Textiles, Zhongyuan University of Technology, 41 Zhongyuan Road, P.O. Box 110, Zhengzhou City 450007, Henan Province, People's Republic of China
e-mail: hejianxin771117@163.com

Introduction

Silk fibroin (SF) has been studied widely as biomedical materials due to its favorable biological compatibility and biodegradability. Surgical sutures, biosensors developed by the enzyme immobilization technique, films with selective permeability, biocompatible devices with controlled drug release, wound-repairing and bone-binding functions are some of the applications already developed or suggested for SF. However, SF needs blending with other macromolecules because of the defaults of pure SF films such as weak strength, frangibility, lack of flexibility, and high solubility in water. Up to now, the blend films of SF with poly(vinyl alcohol) [1], nylon 66 [2], polyurethane [3], and poly(ethylene oxide) [4] have been developed and some properties of SF film were improved, especially mechanical property. However, the biocompatibility of SF would be impaired owing to the additions of these synthetic macromolecules.

It is also an important route for improving SF film by blending with natural macromolecular. Noishiki prepared the SF/cellulose whisker composite films with varied compositions, and their research showed a conformational change of SF from random coil to β-sheet structure induced by the contact of SF molecules with a highly ordered surface of cellulose whisker [5]. This conformational change was also observed in the SF/chitosan blend films, and the investigation of Kweon et al. indicated that the mechanical properties of SF films enhanced by blending 10–40% chitosan and the two compositions were miscible [6]. Similarly, some blend films such as SF/sodium alginate [7], SF/gelatin [8], and SF/S-carboxymethyl kerateine [9] had been prepared using solution blend method, however, there was still absent from detailed description about the mechanism of conformational transition of SF in these blend films.

Carboxymethyl chitosan (CMCS), a derivate of chitosan, has been used in the fields of medicament and food because CMCS keeps the advantage of chitosan and improves its water solubility. The experiment had demonstrated that CMCS avoided the slow biodegradation of chitosan and possessed a higher biosafety [10]; however, there has no report about the SF/CMCS blend film. In this article, the SF/CMCS blend films were prepared, and the effect of CMCS content on the structure and properties of the blend films was investigated, especially the conformational transition of SF induced by blending CMCS was analyzed.

Experimental

Materials

Bombyx mori cocoon came from Henan province, China. CMCS (degree of deacetylating 90.2%; degree of substitution 0.8; viscometric average molecular weight 4.8×10^5) was supplied by Shanghai Chemical reagent Co. Ltd., China. All chemical reagents were analytical reagent.

Preparation of regenerated SF solution

In order to remove the sericin, the cocoons were degummed using 0.5% Na_2CO_3 solution at 98 °C for three times. Degummed SF was washed thoroughly with deionized water for 30 min and then gently dried in air. The dissolution of SF was then performed for 2 h using a ternary solvent system of $CaCl_2$, C_2H_5OH, H_2O with a molar ratio of 1:2:8 by a mechanical stirring. The temperature of dissolution was 75 °C and the liquor ratio was 10:1. The undissolved part was removed by filtration. The fibroin-salt solution was dialyzed against deionized water for 3 days, and a SF solution with a concentration of 2.2% was obtained.

Preparation of SF/CMCS blend films

The CMCS solution with a concentration of 2.2% was prepared by dissolving CMCS in H_2O. SF and CMCS solutions with various ratios were mixed by stirring, and the total mass of two components was controlled at 0.2 g. Finally, the product was cast on polystyrene Petri dish surfaces for 24 h at 40 °C in fan drying, and the thickness of obtained films was about 45 μm. Bend films were balanced at a temperature of 20 °C and a relative humidity of 65% before further measurement.

Scanning electron microscopy

The samples were coated with gold film to observe the surface morphology. The instrument was a JEOL JSM-5600LV electron microscopic with an accelerating voltage of 15 kV.

FTIR spectroscopy

FTIR spectra of the film samples were recorded with a Nicolet Nexus 670 FTIR spectrometer, using the KBr disc technique (1 mg powdered film sample/300 mg KBr). One hundred scans were taken with a resolution of 2 cm^{-1}.

X-ray diffraction analysis

X-ray diffraction was record at room temperature from 5° to 50° at a scanning speed of 0.02°/s with a Rigaku-D/Max-2550PC diffractometer using Ni-filtered Cu K_α radiation of wavelength 0.154 nm. The operating voltage and current were 40 kV and 30 mA, respectively.

DSC analysis

DSC analysis was carried out using a Perkin-Elmer Diamond DSC analyzer under nitrogen gas at a flow rate of 30 mL/min and a heating rate of 10 °C/min.

Measurement of mechanical properties

The mechanical properties of film samples (50 mm × 15 mm) were measured with a stretching speed of 100 mm/min on INSTRON 5582 tensile tester at ambient conditions.

Measurement of moisture absorption and water vapor transmission rate

The blend films with the same size were dried to constant weight at 110 °C after moisture equilibrium at a temperature of 20 °C and a relative humidity of 65%. Moisture content (M) of film was calculated as follows:

$$M = \frac{M_1 - M_2}{M_1} \times 100\%, \tag{1}$$

where M_1 is the balance weight before drying and M_2 the weight after drying.

The cup with 15 mL H_2O covered and sealed with film sample at a temperature of 20 °C was weighed at intervals of 3 h. The original relative humidity in the outside of film was 40%. Water vapor transmission rate of the film was calculated as follows:

$$Q = \frac{w_{i-1} - w_i}{At} \times 100\% \quad (i = 1, 2, \ldots, n), \tag{2}$$

where Q is the water vapor transmission rate of the sample (g/m^2 h), w_i the weight of the cup covered with film sample (g), t the interval time between two weighting (h), and A the useful area of film sample covered on the cup (m^2).

Measurement of solubility in water and swelling capacity

The film samples were dried at 105 °C for 24 h, and the water content in the films was determined. Meanwhile, the films were immersed into 100 mL deionized water at 37 °C for 24 h, prior to be rinsed thoroughly with ethanol, and dried at 105 °C for 24 h. The solubility (D) of blend film in the water was calculated as follows [11]:

$$D = \frac{W_1 - W_2}{W_1} \times 100\%, \tag{3}$$

where D is the solubility in water, W_1 the dry weight of undissolved samples, and W_2 the dry weight of dissolved samples.

The blend films were immersed in water for 24 h at room temperature, and then weighed after moisture at the surface of samples was sucked off. Swelling capacity (S) of blend films was calculated as follows:

$$S = \frac{G_2 - G_1}{G_1} \times 100\%, \tag{4}$$

where G_1 is the dry weight of samples and G_2 the weight of samples immersed in water for 24 h.

Results and discussion

Moisture absorption and water vapor transmission property of blend films

Moisture absorption of blend film is due to the bonding between water molecule and free hydrophilic groups [12]. Figure 1 shows the moisture content of blend films with different CMCS contents. Moisture content of pure SF film was 8.3%. Hydrophilicity of CMCS was more than of SF, and pure CMCS film possessed a moisture content of 10.1%. However, moisture content of SF film reduced from 8.3 to 6.5% with the addition of 5% CMCS. This demonstrated the formation of more intermolecular hydrogen bonds in SF/CMCS blend film, which resulted in the decrease of free hydrophilic groups such as hydroxyl, carboxyl, amido, etc. Only CMCS content increased to 15%, there was an increase in the moisture content of blend film, suggesting more hydrophilic groups were released from the intermolecular hydrogen bonds on the inside of blend film.

As shown in Fig. 2, water vapor transmission rate of blend films with various blend ratios was time dependent, that is, water vapor transmission rate of blend films

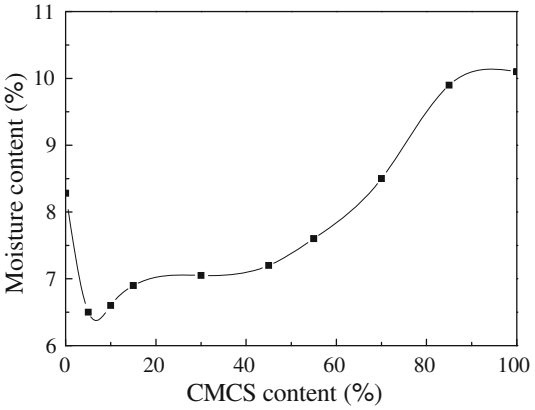

Fig. 1 Moisture contents of blend films with different CMCS contents

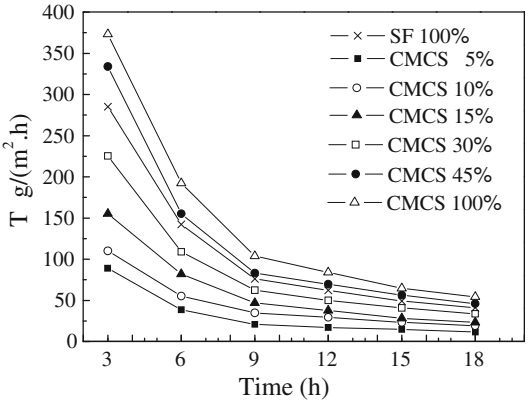

Fig. 2 Vapor transfer rates of blend films with various CMCS contents

decreased apparently before 9 h, and after this, it became stable. However, it can be found that water vapor transmission property of SF film would reduce markedly after adding 5% CMCS, for example, water vapor transmission rate at 3 h decreased from 285 to 89 g/m^2 h. Being similar to moisture absorption, water vapor transmission property of blend film started to increase apparently from adding 15% CMCS. Water vapor transmission property reflects the capacity of water vapor transmitting blend film, which is associated with its crystallinity. The great crystallinity in blend film would make against the permeation of water molecules. Therefore, adding some CMCS could bring on an increase in the crystallinity of SF film, but when CMCS content came to 15%, the reduction in the crystallinity of blend film would occur possibly.

Solubility in water and swelling capacity of blend films

As random coil and silk I (α-helix) of SF can dissolve in water, and Silk II (β-sheet) conformation of SF is insoluble in water, conformational transition can be judged by measuring the weight loss of blend film in water [11]. Figure 3a shows a change curve of the weight loss of blend films with various CMCS content in water. The experimental result indicated that when CMCS content was from 5 to 10%, the blend films were hardly dissolved in water, but pure SF film was almost dissolved in water completely. This demonstrated that the addition of 5–10% CMCS into SF films induced a rather complete transformation of SF molecule to Silk II conformation, a more stable silk form, accordingly, the blend films containing 5–10% CMCS should have a higher crystallinity. When CMCS content increased again, the solubility of blend films increased rapidly, indicating a decrease of the β-sheet SF in blend film when CMCS content came to 15%. The measuring results later provided by X-ray diffraction analysis would also give evidence of this deduction.

As shown in Fig. 3b, there was also lower swelling capacity when CMCS content was 5–10%. Swelling capacity reflects a water retaining capacity of film sample, which is dominated by free hydrophilic groups and free volume in blend film. Correspondingly, swelling capacity of blend films should be affected by their hydrogen bond scale and crystallinities together. The swelling capacity results of SF/CMCS blend films also confirmed our foregoing analysis. When adding 5–10% CMCS into SF film, a large scale of intermolecular hydrogen bonds in blend films resulted in the absence of redundant free hydrophilic groups, and here high crystallinity of blend films made there no interstice to keep and contain water molecules. When CMCS content was more than 15%, swelling capacity of blend films increased obviously, because stores of amorphous region of SF and CMCS held the moisture except that some intermolecular hydrogen bonds of SF and CMCS composed the framework of blend films. When CMCS content exceeded 55%, the framework of blend films composed of a small quality of the intermolecular hydrogen bonds could not prevent the solution of CMCS and SF existing in the large amorphous area, and the swelling capacity of blend films measured reduced.

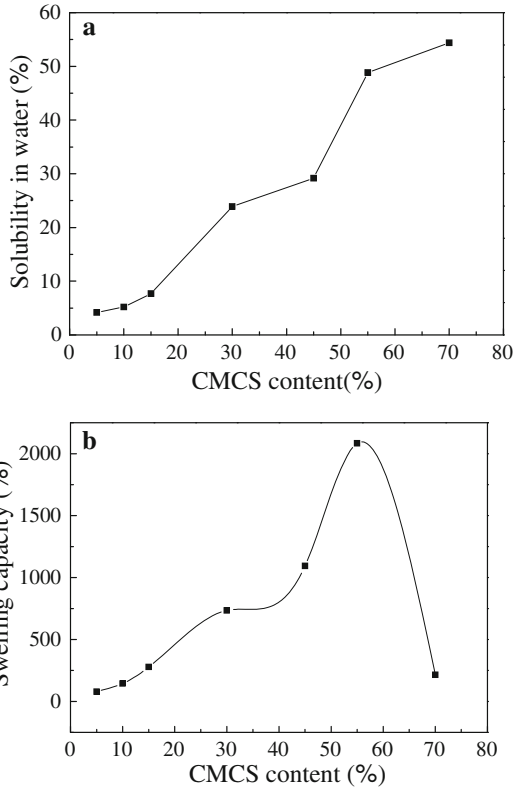

Fig. 3 Solubility in water (**a**) and swelling capacity (**b**) of blend films with various CMCS contents

FTIR spectra analysis

IR spectroscopy is a widely used technique to study the molecular conformation of SF because the amide bands of IR spectra are known to be sensitive to the molecular conformation of SF. FTIR spectra of SF/CMCS blend films with different composition are shown in Fig. 4. Pure SF film showed strong absorption bands at 1655 cm^{-1} (amide I), 1543 cm^{-1} (amide II), and 1240 cm^{-1} (amide III), assigned to α-helix conformation, and only a shoulder at 1527 cm^{-1} (amide II) and 1265 cm^{-1} (amide III), attributed to β-sheet [13]. The blend films gave entirely the different spectra from that of pure SF film in amide region. The blend films with CMCS content up to 45% showed the strong characteristic bands of β-sheet at 1629, 1527, and 1265 cm^{-1}. In addition, after blending with CMCS, there was a decrease in the absorption of SF at 1160 cm^{-1} attributed to the vibration of phenol in Tyr residue, which takes exclusively random coil form [14]. These changes closely correspond to those of X-ray diffraction profile (see later), indicating basic transformation of SF from α-helix or random coil to β-sheet by blending with CMCS.

When adding 5% CMCS into SF film, SF exhibited a complicated band in amide I region, which composed of a sharp peak at 1629 cm^{-1} and a shoulder peak at

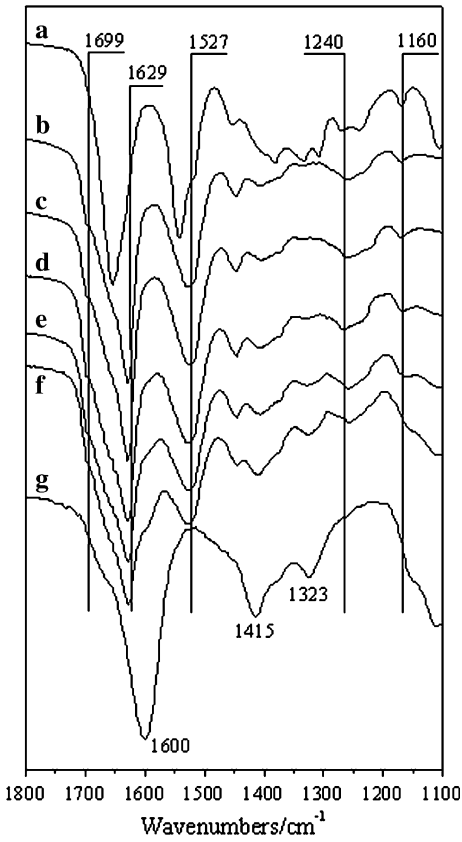

Fig. 4 FTIR spectra of (*a*) pure SF film, blend films containing (*b*) 5%, (*c*) 10%, (*d*) 15%, (*e*) 30% and (*f*) 45% CMCS, and (*g*) pure CMCS film

1699 cm^{-1}, assigned to β-sheet conformation; and only a weak absorption remained at 1655 cm^{-1}, assigned to α-helix conformation (Fig. 4b). When CMCS content in blend film increased further, the peak intensities at 1629 and 1699 cm^{-1} reduced, indicating a most complete transformation of SF to β-sheet conformation occurred in the blend film with 5% CMCS.

It is well accepted that spectral shifts of small magnitude provide a useful criterion for miscibility and also give the information about the nature of the specific interaction in a variety of blends [15]. The characteristic absorption peaks of CMCS film were presented at 1600, 1413, and 1323 cm^{-1} (Fig. 4g), assigned to the C=O stretching, the C–O stretching of carboxyl group, and the C–N stretching. In the SF/CMCS blend films, the C=O stretching band of CMCS disappeared, and with the decrease of CMCS content, the C–O stretching of carboxyl group of CMCS shifted to lower wave number, whereas the C–N stretching of CMCS shifted to slightly higher wave number. From the observation of the spectral shift of CMCS, the interaction between SF and CMCS involved the carboxyl and amino groups of CMCS and the amide of SF. Further, it is noteworthy that only when CMCS content reached 15%, a shoulder peak at about 1600 cm^{-1} appeared gradually, and the peak intensities at about 1413 and 1323 cm^{-1} increased evidently. Therefore, there

would be a two-phase structure in TSF/CMCS blend systems with 15% CMCS or more; however, the two polymers might be supposed to exhibit the miscible blending to a certain extent because of the interaction between SF and CMCS, proved by the band shifts of CMCS in the blend films.

X-ray diffraction analysis

As shown in Fig. 5f, no marked crystalline diffraction peak was found in the X-ray curve of pure CMCS film, suggesting an amorphous structure in pure CMCS film. Generally, there have two types of crystalline structures proposed for SF, i.e., Silk I (α- helix) and Silk II (β-sheet). The main diffraction peaks of Silk I present at around $2\theta = 12.2°$ and 28.3°, while the peaks of Silk II present at about $2\theta = 18.9°$ and 20.7° [16]. Pure SF film showed a wide peak (Fig. 5e), expressing a dominant amorphous structure (random coil).

A conspicuous change in XRD pattern of SF film occurred after adding 5% CMCS. A high-intensity diffraction peak at 2θ angle of 18.9° and two small reflect peaks at 9.1° and 28.3° could be observed (Fig. 5a), among which the peaks at 2θ angle of 18.9° and 9.1° were attributed to silk II, and the peak at 28.3° was the characteristic peak of Silk I. The XRD pattern indicated that the crystalline structures of Silk I and Silk II were coexisted in the blend film containing 5% CMCS, and the Silk II crystalline structure was dominant judging from the relative intensities of the peaks attributed to the two crystalline structures. When CMCS content increased to 10%, the intensity of the peaks at 2θ of 18.9° and 9.1° decreased, whereas the diffraction at 2θ of 28.3° enhanced (Fig. 5b), indicating a conformational transition from β-sheet to α-helix. When CMCS content continued to increase to 15%, the diffraction peaks assigned to Silk I and Silk II reduced or disappeared (Fig. 5c), indicating that SF conformation began to transform to random coil and the crystallinity of blend film decreased obviously. The result of X-ray diffraction analysis was consistent with the conclusion drew in the previous analysis for the properties of blend films.

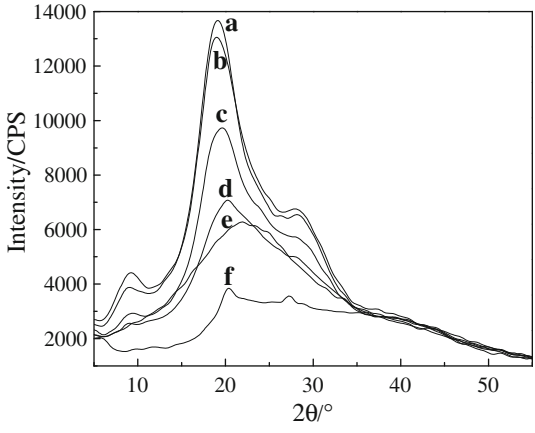

Fig. 5 X-ray diffraction curves of blend films with (*a*) 5%, (*b*) 10%, (*c*) 15% and (*d*) 45% CMCS; (*e*) pure SF film and (*f*) pure CMCS film

Silk fibroin contains at least two major fibroin proteins, light and heavy chains, 25 and 350 kDa, respectively. Considering the peptide sequence of the heavy chain, which account for 95% of total fibroin proteins, this chain can be divided into two blocks, i.e., smaller hydrophilic blocks and larger hydrophobic blocks [17]. In general, these two blocks alternatively connected to each other with larger hydrophilic blocks at the chain ends. Kaplan and Jin suggested that this polypeptide structure could result in the formation of micellar structures by self-assembly which exhibited typical size in the range of 100–200 nm in diameter [18].

As mentioned before, only 5% CMCS could induce a rather complete transition of SF from random coil to β-sheet, here the CMCS:SF was 1:20. Thus, it should not happen for the case of parallel arranging of two polymer molecules alternately to form intermolecular hydrogen bonds and here the ratio of the both polymers should be adjacent to 1:1. However, the fact can be well explained by the model proposed as shown in Fig. 6a. CMCS molecules could use as the nucleus of SF micelles and induced the SF assembly by forming intermolecular hydrogen bonds between the carboxyl, amido, hydroxyl groups of CMCS and the hydrophilic blocks of SF molecule. At the same time, the lager hydrophobic blocks of SF molecules folded to form β-sheet structure during SF self-assembly.

In addition, there occurred a transition from β-sheet to α-helix conformation when CMCS content in blend film reached 10%, indicating that the CMCS content

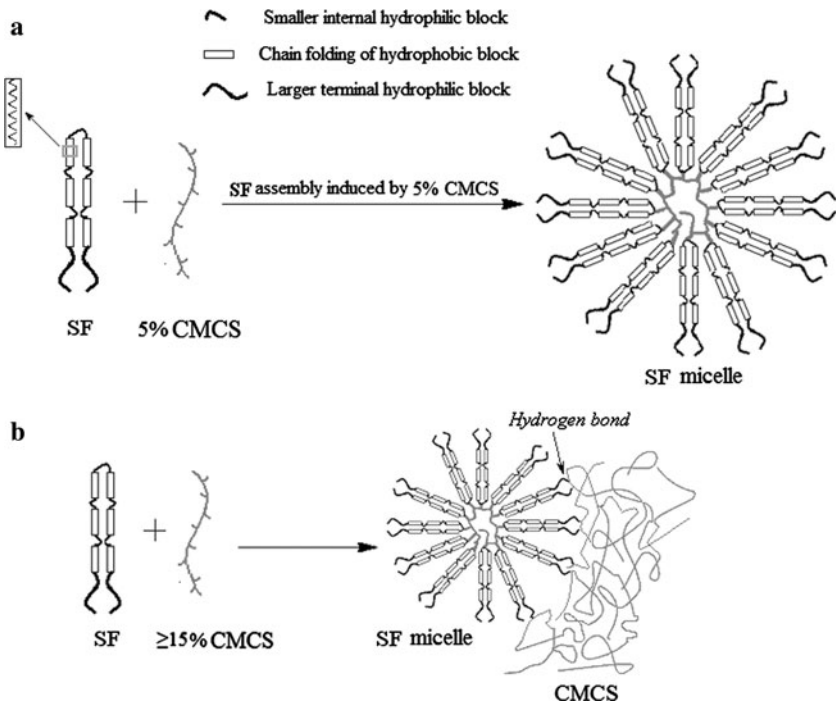

Fig. 6 Models of the interaction between SF and CMCS in the blend films

exceeded the saturation content of CMCS needed for inducing SF self-assembly. With CMCS content adding to 15%, excessive CMCS molecules as amorphous region distributed around SF micelles in the blend film because CMCS chains could not fold themselves to form ordered structure during casting to form a film [15], accordingly, there was a two-phase structure in the blend film, as indicated by IR analysis (Fig. 6b). However, the intermolecular interaction between the two polymers in blend films with 15% CMCS or more still existed in their amorphous parts, as analyzed in IR spectra. Therefore, it demonstrated that in the case of blend films with 15% CMCS or more, the miscibility of SF and CMCS occurred in some intermediate between the miscible blend and phase separation, i.e., the so-called semi-miscible. Furthermore, blending excessive CMCS would make the aggregation of SF molecules in the blend film become difficult due to the interaction of two kinds of molecules and cause local accumulation of SF molecules. Of course, the size and the integrality of aggregated fibroin proteins would decrease, which could reflect from the significant reduction of the β-sheet structure and the crystallinity in blend film.

Thermal behavior

The thermal behavior of SF/CMCS blend films was investigated by means of DSC measurement (Fig. 7). The pure SF film showed the pattern of amorphous SF with three characteristic thermal transitions (Fig. 7a) [19]. An endothermic shift at about 178 °C marked the glass transition (T_g), following by an exothermic peak at 235 °C and a prominent endothermic peak at 280 °C, attributed to the structure transition of SF from random coil to β-structure and the thermal decomposition of SF with unoriented β-sheet structure, respectively. In addition, the endothermic peak at the temperature of 70–90 °C should be associated with moisture evaporation.

The SF/CMCS blend films displayed different thermal behavior from pure SF film. In case of blend film containing 5% CMCS, the characteristic peaks of pure SF film attributed to glass transition and β-sheet crystallization disappeared, and the decomposition peak (T_d) of SF enhanced and shifted up from 280 to 283 °C (Fig. 7b). In addition, the endothermic peak attributed to moisture evaporation showed a clear downward shift from 79 to 70 °C. When CMCS content in blend film increased to 10%, blend film did not show major change in thermal behavior, whereas the T_d of SF decreased and the endothermic peak of moisture evaporation shifted up from 70 to 74 °C (Fig. 7c). This means that a rather complete conformation transition from random coil to β-sheet occurred in the SF film by adding only 5% CMCS. The downward shift of the endothermic peak of moisture evaporation in case of blend film containing 5% CMCS may be due to the structure change of SF from random coil to β-sheet, which enhanced the intermolecular hydrogen bonds between SF molecules and decreased the interaction between SF and water molecules.

With CMCS increased to 15%, the decomposition peak of SF reduced evidently in intensity and shifted downward, accompanied by a weak exothermic peak appeared at 23 °C (Fig. 7d). It could be determined from the thermal behavior of blend films that the reduction of the β-sheet structure of SF in blend film with 15%

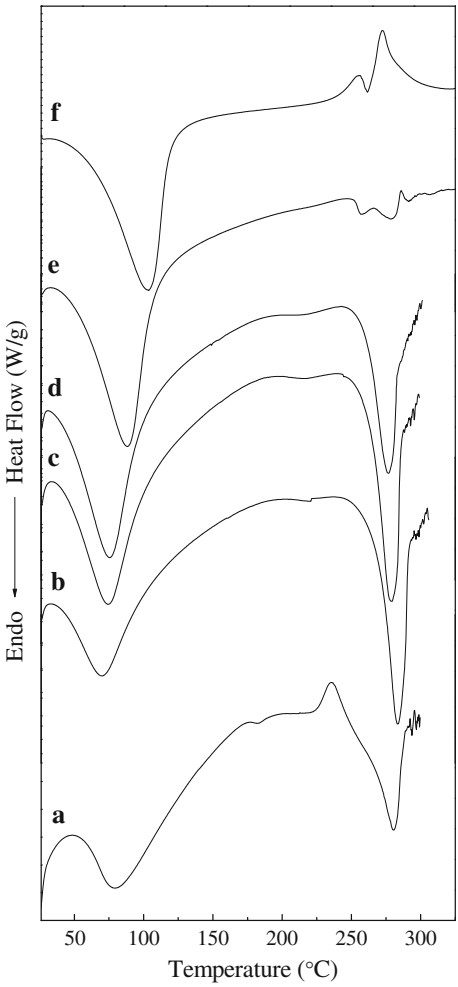

Fig. 7 DSC curves of (*a*) pure SF film, blend films containing (*b*) 5%, (*c*) 10%, (*d*) 15% and (*e*) 45% CMCS, and (*f*) pure CMCS film

CMCS should be more apparent, in good agreement with the above discussed X-ray diffraction results. The DSC curve of blend film with 45% CMCS showed a mixed form of the two components (Fig. 7e), indicating an obvious two-phase structure in the blend film.

Morphological characteristics

The surfaces of pure and blend films were observed by SEM as shown in Fig. 8. The pure SF and CMCS films showed a smooth surface structure; however, the morphology of blend film was dependent on the mixing ratio of SF/CMCS. Blend film with 5% CMCS exhibited a compatible compact texture with random lines appearing throughout the film surface as a result of the contraction of SF after

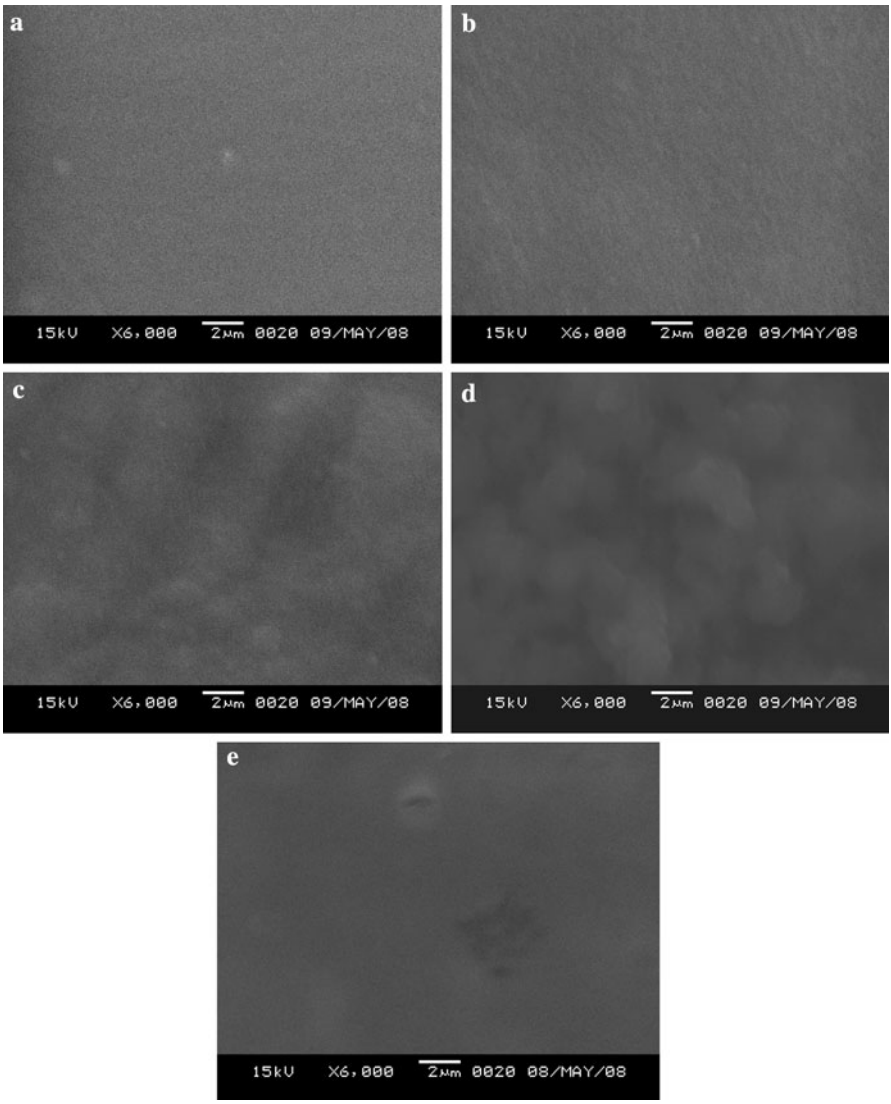

Fig. 8 SEM micrographs of the surface of (**a**) pure SF film, blend films containing (**b**) 5%, (**c**) 15% and (**d**) 45% CMCS, and (**e**) pure CMCS film

conformation transition induced by CMCS (Fig. 8b), but the rough surface with strip structure was observed in the blend film containing 15% CMCS (Fig. 8c). When CMCS content came to 45%, the blend film presented a rougher surface with irregular globular structure (Fig. 8d). From these results, it can conclude that the two polymers gave rise to separated phase in the blend films with 15% CMCS or more, which accorded with the two-phase structure given in above X-ray diffraction analysis.

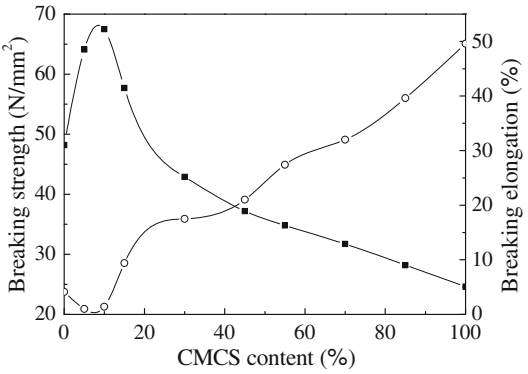

Fig. 9 Mechanical properties of blend films with various CMCS contents

Mechanical properties

Figure 9 presents the change in mechanical properties of blend films with various CMCS contents. With adding CMCS into SF film, there had an increase in the breaking strength of blend films at the beginning, and only CMCS content increased to 15%, the decrease of the breaking strength could be observed, on the other hand, just the reverse for the breaking elongation of blend films. When CMCS content was 15%, the blend film had a higher strength and a lower modulus compared with pure SF film, and the flexibility of the film was improved. Here CMCS content was consistent with the content at which SF molecule transformed to random coil, and prior to this point the high crystallinity resulted in by CMCS inducing SF conformation transition promoted the rigidity of blend films.

Conclusion

The results of FTIR spectra, X-ray diffraction, and DSC analysis demonstrated a rather complete conformation transition of SF from random coil to β-sheet by adding 5% CMCS, and the crystallinity of blend film was maximal, mainly because CMCS molecules could be used as the nucleus of SF micelles and induced the SF assembly by forming intermolecular hydrogen bonds. The conformation of SF in blend film showed a transformation from β-sheet to random coil and the crystallinity of blend film decreased evidently when CMCS content came to 15%. The blend films with 15% CMCS or more presented a two-phase structure, which was proved by SEM observation. However, IR spectra analysis indicated that the intermolecular interaction between the two polymers still existed in blend films with 15% CMCS or more. The blend films displayed the lower moisture absorption, hot-water dissolving rate and swelling rate when CMCS content was less than 15%, and only CMCS content was up to 15%, the values of these properties increased. The blend films with 5 and 10% CMCS showed a rigid structure, however, when CMCS content reached 15%, the breaking strength of blend film began to decrease, whereas the breaking elongation increased.

Acknowledgments The research was financially supported by China Postdoctoral Science Foundation funded project (20080430079, 200902194). We also acknowledge the support from the Programme of Introducing Talents of Discipline to Universities, B07024, China.

References

1. Tanaka T, Suzuki M, Kuranuki N, Tanigami T, Yamaura K (1997) Properties of silk fibroin/poly(vinylalcohol) blend solutions and peculiar structure found in heterogeneous blend films. Polym Int 42:107–111
2. Liu Y, Shao Z, Zhou P, Chen X (2004) Thermal and crystalline behavior of silk fibroin/nylon 66 blend films. Polymer 45:7705–7710
3. Freddi G, Tsukada M, Beretta S (1999) Structure and physical properties of silk fibroin/polyacrylamide blend films. J Appl Polym Sci 71:1563–1571
4. Jin HJ, Park J, Valluzzi R, Cebe P, Kaplan DL (2004) Biomaterial films of *Bombyx mori* silk fibroin with poly(ethylene oxide). Biomacromolecules 5:711–717
5. Noishiki Y, Nishiyama Y, Wada M, Kuga S, Magoshi J (2002) Mechanical properties of silk fibroin–microcrystalline cellulose composite films. J Appl Polym Sci 86:3425–3429
6. Kweon H, Ha HC, Um IC, Park YH (2001) Physical properties of silk fibroin/chitosan blend films. J Appl Polym Sci 80:928–934
7. Liang CX, Hirabayashi K (1992) Improvements of the physical properties of fibroin membranes with sodium alginate. J Appl Polym Sci 45:1937–1943
8. Gil ES, Frankowski DJ, Hudson SM, Spontak RJ (2007) Silk fibroin membranes from solvent-crystallized silk fibroin/gelatin blends: effects of blend and solvent composition. Mater Sci Eng C 27:426–431
9. Lee KY, Ha WS (1999) DSC studies on bound water in silk fibroin/S-carboxymethyl kerateine blend films. Polymer 40:4131–4134
10. Jung KL, Soo U, Jung HK (1999) Modification of chitosan to improve its hypocholesterolemic capacity. Biosci Biotechnol Biochem 63:833–838
11. Feng XX, Zhang LL, Chen JY (2007) Preparation and characterization of novel nanocomposite films formed from silk fibroin and nano-TiO_2. Int J Biol Macromol 40:105–111
12. Agarwal N, Hoagland DA, Farris RJ (1997) Effect of moisture absorption on the thermal properties of *Bombyx mori* silk fibroin films. J Appl Polym Sci 63:401–410
13. Freddi G, Monti P, Nagura M, Gotoh Y, Tsukada M (1997) Structure and molecular conformation of tussah silk fibroin films: effect of heat treatment. J Polym Sci B 35:841–847
14. Arp Z, Autrey D, Laane J, Overman SA (2001) Tyrosine Raman signatures of the filamentous virus Ff are diagnostic of non-hydrogen-bonded phenoxyls: demonstration by Raman and infrared spectroscopy of p-cresol vapor. Biochemistry 40:2522–2529
15. Panya W, Yasuhiko T, Ratana R (2007) Miscibility and biodegradability of silk fibroin/carboxymethyl chitin blend films. Macromol Biosci 7:1258–1271
16. Liang CX, Hirabayashi K (1992) Influence of solvation temperature on the molecular features and physical properties of fibroin membrane. Polymer 33:4388–4393
17. Inoue S, Tanaka K, Tanaka H (2004) Assembly of the silk fibroin elementary unit in endoplasmic reticulum and a role of L-chain for protection of 1,2-mannose residues in N-linked oligosaccharide chains of fibrohexamerin/P25. Eur J Biochem 271:356–366
18. Jin HJ, Kaplan DL (2003) Mechanism of silk processing in insects and spiders. Nature 424: 1057–1061
19. Magoshi J, Nakamura S (1975) Physical properties and structure of silk: glass transition and crystallization of silk fibroin. J Appl Polym Sci 19:1013–1019